ACS APPLIED BIO MATERIALS

www.acsabm.org Article

Cold Plasma Discharge Tube Enhances Antitumoral Efficacy of Temozolomide

Xiaoliang Yao,[†] Dayun Yan,[*,†] Li Lin, Jonathan H. Sherman, Katherine B. Peters, Stephen T. Keir, and Michael Keidar[*]

Cite This: https://doi.org/10.1021/acsabm.2c00018 Read Online

ACCESS | Metrics & More | Article Recommendations | Supporting Information

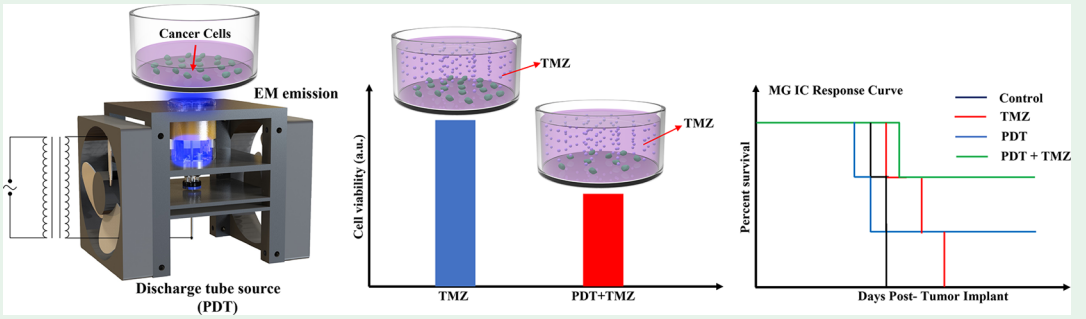

ABSTRACT: Glioblastoma (GBM) is a fatal human brain tumor with a low survival rate. Temozolomide (TMZ) has been widely used in GBM therapy with noticeable side effects. Cold plasma is an ionized gas that is generated near room temperature. Here, we demonstrated the enhancement therapeutic efficacy of TMZ via using a cold plasma source based on nonequilibrium plasma in a sealed glass tube, named a radial cold plasma discharge tube (PDT). The PDT affected glioblastoma cells' function just by its electromagnetic (EM) emission rather than any chemical factors in the plasma. The PDT selectively increased the cytotoxicity of TMZ on two typical glioblastoma cell lines, U87MG and A172, compared with normal astrocyte cell line hTERT/E6/E7 to some extent. Furthermore, on the basis of a patient-derived xenograft model, our preliminary in vivo studies demonstrated the drastically improved mean survival days of the tumor-barrier mice by more than 100% compared to control. The PDT is not only independent of continuous helium supply but is also capable of resisting the interference of environmental changes. Thus, the PDT was a stable and low-cost cold atmospheric plasma source. In short, this study is the first to demonstrate the promising application of PDTs in GBM therapy as a noninvasive and portable modality.

KEYWORDS: *plasma discharge tube, antitumor, glioblastoma, Temozolomide, drug-sensitization*

Downloaded via GEORGE WASHINGTON UNIV on March 28, 2022 at 13:43:38 (UTC).
See https://pubs.acs.org/sharingguidelines for options on how to legitimately share published articles.

INTRODUCTION

Cold plasma is an ionized gas generated at room temperature and under atmospheric pressure conditions that contains electrons, ions, neutral particles, ultraviolet (UV) emission, and EM effect.[1−4] Chemical components, particularly reactive species in cold atmospheric plasma have been regarded as the key players in the biological response of cells and tissues to both direct and indirect treatment.[5,6] In particular, promising cold plasma-based cancer therapy has been largely regarded as that based on reactive oxygen species (ROS) and reactive nitrogen species (RNS).[7−9] However, the potential role of physical factors in cold plasma has been ignored, mainly because of a lack of direct experimental demonstration of any cellular responses.[10,11]

Recently, a novel experiment demonstrated that the strong anticancer capability of cold plasma treatment based on physical factors, probably just the EM effect, was observed in six cell lines, including brain cancer cells, bladder cancer cells, and melanoma cells.[12−14] The EM effect in cold plasma has at least three advantages compared with chemical factors in terms of antitumoral performance: the trans-barrier nature, the reactive-species-independent nature, and the necrotic fate of the damaged cells.[12] The trans-barrier nature means the physical factors in cold plasma can affect cells through a physical barrier and provide a routine to kill cells in a contactless way. The reactive-species-independent nature means that physical factors can also kill reactive-species-resistant cancer cells.

Previous demonstration of physically based treatment was based on traditional cold plasma source design. Here, we

Received: January 9, 2022
Accepted: March 13, 2022

© XXXX American Chemical Society

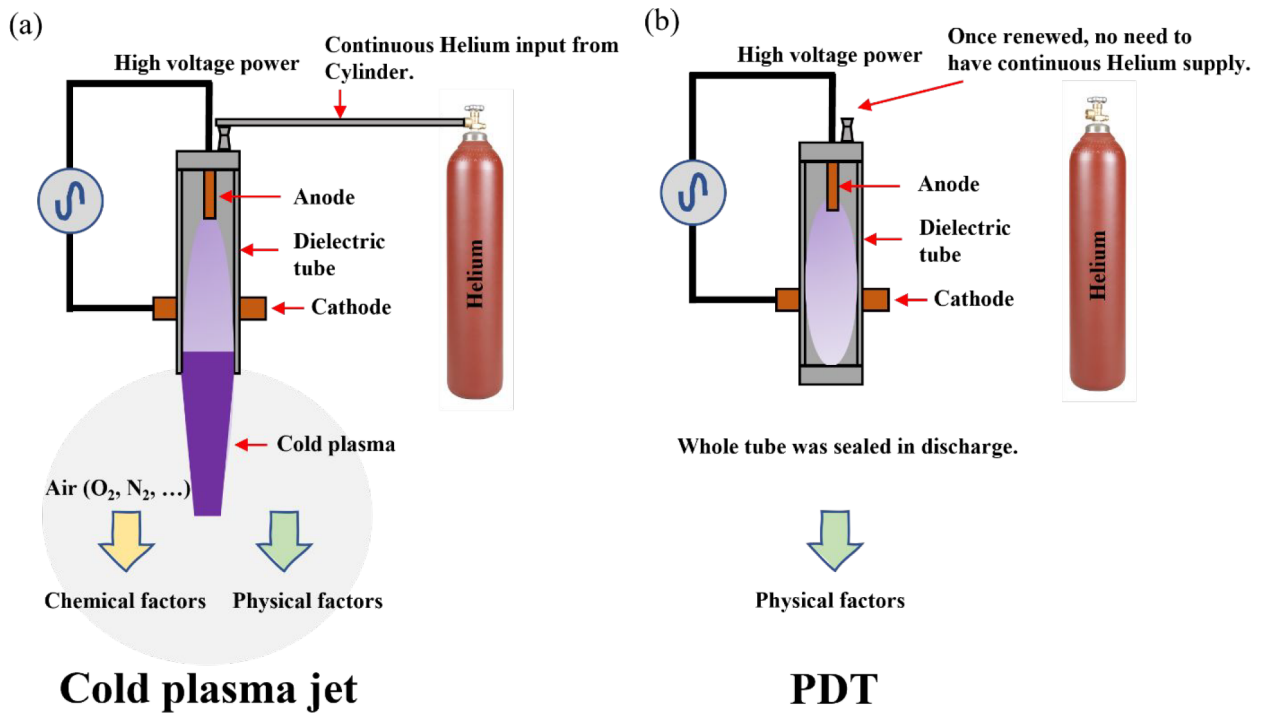

Figure 1. Schematic illustration of the basic design of two cold plasma sources. (a) Cold plasma jet source: both chemical factors and physical factors can affect targets. However, the contact blockage between the plasma body with targets can filter all chemical factors. (b) PDT source: only physical factors can affect targets.

demonstrate the promising antitumoral capability by a novel designed low-cost source, a radial cold plasma discharge tube (PDT). The fundamental difference between a PDT and a cold plasma jet is illustrated here. Take a helium-based cold plasma jet as an example. Its discharge occurs in an environment that contains both helium and air components such as oxygen (O_2) and nitrogen (N_2) (Figure 1a). Helium flow is necessary to sustain the continuous generation of the cold plasma jet. Thus, plenty of helium input is necessary, which results in a high research cost for the cold plasma jet. In addition, environmental factors (environmental gas composition, humidity, and airflow) drastically affect the stability and composition of the cold plasma jet in operation.[15] Another vital concern is that the continuous gas flow cannot be accepted when a cold plasma treatment needs to be performed in a tissue with very limited space, such as in the bladder or in other organs. The sealed space in PDT overcomes all these dilemmas simultaneously (Figure 1b). The discharge occurred only in an isolated space. Once helium gas has been renewed, it can be used multiple times until there is helium leakage, which a better sealing approach can improve. Obviously, only physical factors in PDT are allowed to affect cells or tissues, and more importantly, in a contactless way. Thus, PDT is also a prototype of a wearable device such as a treatment helmet. More attractively, PDT can be made into a tiny size, even at the micro- or submicrometer scale, which is a prototype of a micro/nano cold plasma source and might have wide application in nanomedicine with the help of a nanogenerator.[16]

Glioblastoma (GBM) is the most common, malignant, and fatal human brain tumor. Most patients pass away within a year after diagnosis.[17] Temozolomide (TMZ) is a widely used oral alkylating agent to treat GBM.[18] TMZ has advantages over other existing alkylating agents because of its unique chemical structure and pharmacokinetic properties. For example, TMZ can cross the blood−brain barrier because of its low molecular weight.[19] However, TMZ works for less than 50% of patients, with noticeable side effects, such as vomiting and nausea.[20] Thus, there is a clear need to find novel approaches to simultaneously improve the efficacy of TMZ while reducing its side effects, particularly the damage on normal cells.[21]

Here, we demonstrated that a PDT source could cause growth inhibition on glioblastoma cell lines and enhance the antitumoral capability of TMZ in vitro and in vivo. In particular, in vivo studies were performed on an intracranial tumor xenografted model, which was based on a primary patient-derived GBM xenograft model. Compared to previous studies using established cell lines, this work shined more light to its translational and clinical potentiality. Furthermore, PDT-TMZ treatment caused noticeable weaker growth inhibition on normal astrocytes than cancer cell lines, which suggests PDT is a promising modality to improve the side effect of TMZ. PDT treatment was performed in a contactless approach, which shines a light on the probability of using PDT as a noninvasive antitumoral modality in the future.

METHODS AND MATERIALS

Radial PDT Setup. The PDT source was mainly composed of a cylinder quartz glass tube (ACS Pharma) filled with pure helium (99.995% purity, Roberts Oxygen, grade 4.5, size 300), where two electrodes triggered the discharge with a voltage of 5.8 kV and a frequency of 12.5 kHz (Figure 2a). The cylinder glass tube had a radius of 21.5 mm and a height of 85 mm. The central anode had a radius of 2 mm. The annular cathode had a radius of 21 mm and a height of 20 mm. Two 12 V DC cooling exhaust fans (GOSTIME) were added at both sides to inhibit overheating (Figure 2b, c). The temperature on the top center of the PDT was measured using a Hti-HT-02D hand-held digital infrared thermal imaging camera thermometer, where 24-well plates were placed. The bottom temperature of the 24-well plate increased from 24 to 31 °C after 7

https://doi.org/10.1021/acsabm.2c00018
ACS Appl. Bio Mater. XXXX, XXX, XXX−XXX

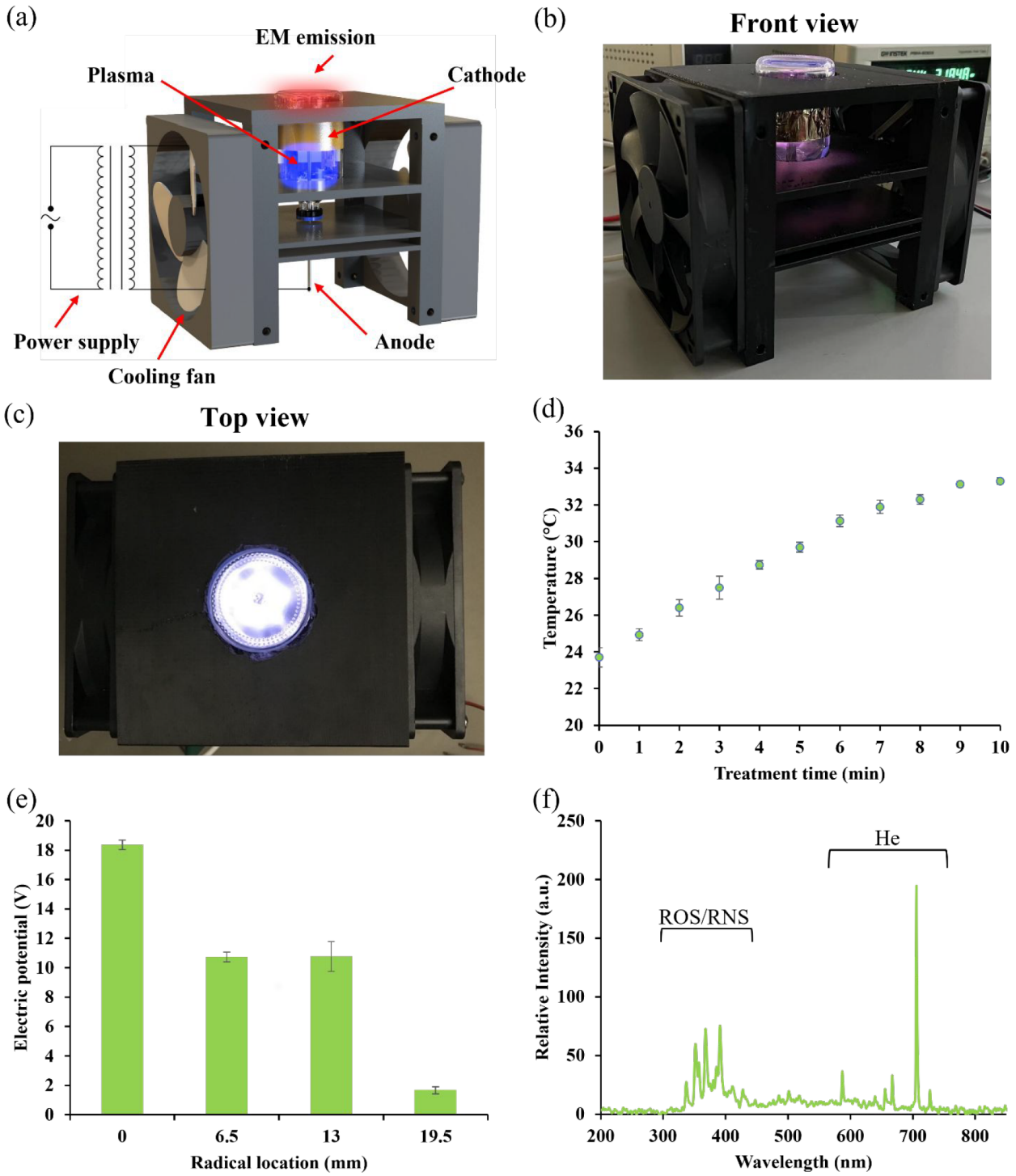

Figure 2. PDT source. (a) Schematic illustration of PDT source. (b) Front view. (c) Top view. (d) Heating effect of PDT treatment on a 24-well plate (n = 5). (e) Electric potential distribution of PDT: from the center to the edge (n = 5). (f) OES of plasma in PDT with a voltage of 5.8 kV and a frequency of 12.5 kHz.

min of treatment (Figure 2d). Even when the treatment time was increased to 10 min, the bottom temperature of the plate was lower than 35 °C, which is still lower than the standard cell culture temperature of 37 °C. Obviously, the heating effect of PDT will not affect cells. The electric potential distribution was measured by probes placed on the top surface of PDT, which gradually decreased toward the top radial edge (Figure 2e). The plasma composition in PDT was characterized by optical emission spectroscopy (OES, StellarNet EPP2000). As shown in Figure 2f, a typical spectrum has the largest peak between 500 and 750 nm, corresponding to helium components. In contrast, there are only weak peaks between 300 and 400 nm, corresponding to ROS/RNS components in plasma. UV generation from cold plasma is very weak, which has been demonstrated in previous studies.[12,22] Thus, the ignorable UV generation in PDT will not affect cells.

Cell Culture and PDT Treatment. Human glioblastoma cell lines U87MG and A172 and human astrocyte cell line hTERT/E6/E7 cells were obtained from ATCC (Manassas, VA) and cultured in DMEM (Gibco, 11965118) supplemented with 10% (v/v) fetal bovine serum (Atlantic Biologicals, S11150) and 5% (v/v) penicillin-streptomycin

https://doi.org/10.1021/acsabm.2c00018
ACS Appl. Bio Mater. XXXX, XXX, XXX−XXX

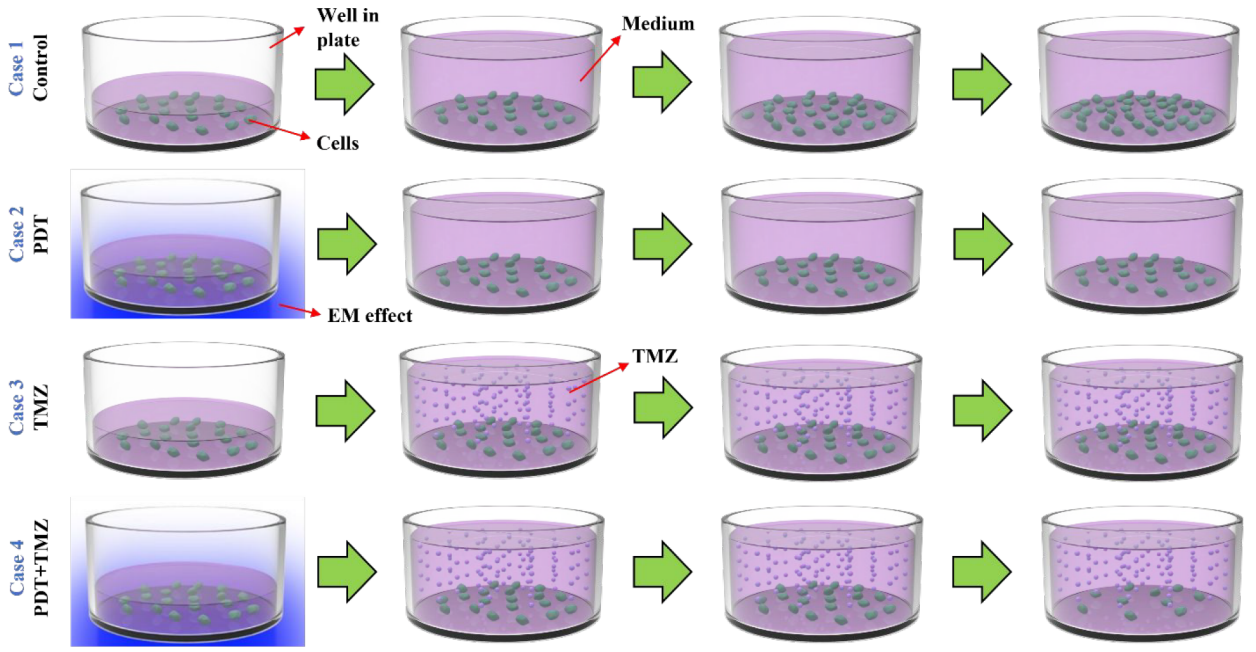

Figure 3. Basic research strategy. Cases 1, 2, 3, and 4 are named as Control, PDT, TMZ, and PDT + TMZ, respectively. Such appellation was used throughout the whole study. EM emission was generated from the PDT source underneath.

solution (Life Technologies, 15140122) under standard culture conditions (37 °C, a humidified, 5% CO_2/95% air environment). Temozolomide was purchased from Life Sciences (ALX-420-044; Farmingdale, NY). The entire study was performed on the basis of four cases (Figure 3): case 1, control, in which neither PDT treatment nor TMZ treatment was performed on cells; case 2, PDT treatment (1, 4, 7 min) alone, which included PDT-only treated cells without TMZ treatment; case 3, TMZ treatment alone, in which cells were only treated by TMZ (Enzo life science, 400 μM) without PDT treatment; and case 4, TMZ (400 μM) treatment on the PDT-treated cells. For a typical PDT treatment (1, 4, 7 min), 1.5×10^4 cells/well were seeded in a 24-well plate for 24 h. Before PDT treatment, the overnight supernatant was replaced by 20 μL/well fresh DMEM. After treatment, the medium was replaced by 500 μL/well fresh DMEM or DMEM containing TMZ, followed by 72 h of culture before the final cell viability assay using thiazolyl-blue tetrazolium bromide (MTT) (Sigma-Aldrich, M2128). The absorbance at 570 nm was read using an H1 multifunction microplate reader (Hybrid Technology). All cell viability data were normalized by the division between the experimental and control groups.

Fluorescent Dye. Cells were gently resuspended in the suitable dyes and incubated for 45 min at 37 °C. Cells were then centrifugated to remove CellTracker (Invitrogen) working solution. In monoculture case, 5000/well U87 cells or hTERT/E6/E7 cells were seeded in 96-well plates for 24 h. In the coculture case, the mixture of 5000/well E6E7 cells and 5000/well U87 cells were cultured in 96-well plates for 24 h. Relative fluorescence units (RFU) were measured using a Synergy H1 Hybrid multimode microplate reader 72 h after treatment. The final fluorescence data were normalized by the division between the experimental and control groups.

Animal Studies. Female athymic mice (nu/nu genotype, Balb/c background, 6–8 weeks old) were used for in vivo antitumor study. Animals were maintained in filter top cages in Thoren units (Thoren Caging Systems, Inc., Hazelton, PA). All animal procedures conformed to Institutional Animal Care and Use Committee and National Institute of Health guidelines.

Tumor Xenograft and Implantation. D09-0394MG, a patient-derived human GBM xenograft line, was used for this intracranial study. This line was established and maintained at the Preston Robert Tisch Brain Tumor Center at Duke University. For intracranial studies, subcutaneous xenografts passaged in athymic mice were excised from host mice under sterile conditions in a laminar flow containment hood. The xenograft was minced, and cells were separated with a 60-mesh tissue cytosieve (BioWhittaker Inc., Walkersville, MD) into a Zinc Option solution (Sigma-Aldrich, Allentown, PA), allowing for passage through a 25-gauge needle. After centrifugation, supernatant was removed, and cells were mixed 1:1 with methylcellulose. This mixture was then loaded into a repeating 250-/J Hamilton syringe (Hamilton, Co., Reno, NV) dispenser and injected intracranial into the right cerebral hemisphere of the athymic mouse at an inoculation volume of 5 μL. The intracranial injections were done by placing a mouse into a stereotactic frame. A 1/2 in. midline skin incision was made. The bregma served as the point of origin for the coordinate system when an intracranial injection was performed. The injection site was 0.5 mm anterior and 2 mm lateral of the bregma. Once at that point, the needle was inserted into the brain 3.7 mm. The needle was then pulled back up to 3.4 mm deep. This created a well for the injection. The bregma was located and the coordinates (2 mm lateral) determined (Figure S1). A mounting holder on the frame held the syringe containing the cells. A sterile 25-gauge needle attached to the syringe was introduced through the calvaria and into the brain at a depth of 3.5 mm. The xenograft homogenate was injected, the syringe was pulled up after 1 min, and a small amount of bone wax was placed to occlude the hole. The mouse was removed from the frame and surgical glue was used to close the skin. Lidocaine and bupivicaine were used to control for pain.[23]

RESULTS

Enhancing TMZ's Cytotoxicity. PDT treatment has shown a remarkable enhancing effect on TMZ's efficacy. The PDT just caused a weak impact on two cell lines. For U87MG cells, the PDT alone decreased cell viability by 4, 13, and 31%, respectively (Figure 4a). TMZ (400 μM) alone decreased the cell viability by 18%. In contrast, TMZ could cause a decreased cell viability on the PDT-treated (1, 4, 7 min) cells of 25, 34, and 55%, respectively (Figure 4b). For A172 cells, a similar trend has also been observed. PDT alone (1, 4, 7 min) decreased the cell viability by 2, 15, and 28%, respectively (Figure 4c). TMZ alone decreased cell viability by 20%. In contrast, the TMZ treatment on the PDT-treated (1, 4, 7 min) cells decreased cell viability by 27, 33, and 58%, respectively

https://doi.org/10.1021/acsabm.2c00018
ACS Appl. Bio Mater. XXXX, XXX, XXX–XXX

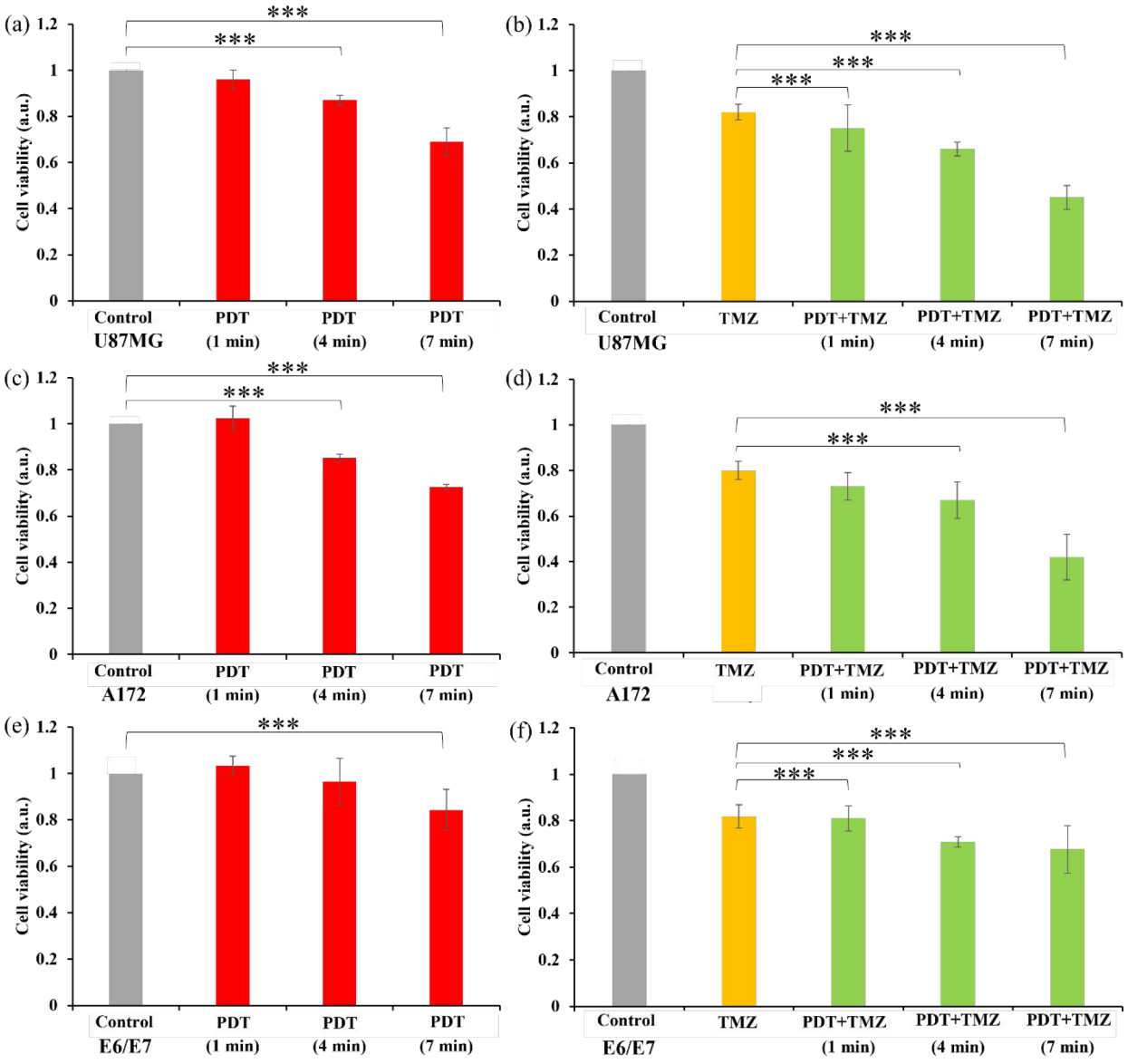

Figure 4. Enhanced cytotoxicity of TMZ by PDT. (a) U87MG cells after PDT treatment. (b) U87MG cells after PDT + TMZ treatment. (c) A172 cells after PDT treatment. (d) A172 cells after PDT + TMZ treatment. (e) hTERT/E6/E7 cells after PDT treatment. (f) hTERT/E6/E7 cells after PDT + TMZ treatment. A student's *t* test was performed, and statistical significance was indicated as * $p < 0.05$, ** $p < 0.01$, *** $p < 0.001$ ($n = 5$).

(Figure 4d). More importantly, the PDT just shows a much weaker effect on normal astrocyte hTERT/E6/E7. The PDT alone (1, 4, 7 min) caused a weak effect on hTERT/E6/E7 cells via decreasing cell viability by 3, 3.5, and 15%, respectively (Figure 4e). TMZ alone decreased cell viability by 19%. The pretreatment of PDT caused a decreased cell viability of 19, 30, and 33%, respectively (Figure 4f). Obviously, via the physical factors in PDT, the cytotoxicity of TMZ could be more strongly enhanced in glioblastoma cells than in normal astrocytes.

PDT's in vivo effect has been studied using an intracranial xenograft model. The schematic illustration is presented in panels a and b in Figure 5. Groups of three mice were randomized into the following groups 10 days post tumor implantation: vehicle control group, "TMZ alone" group, "PDT alone" group, and "combination" (PDT+TMZ) group. TMZ was administered IP using a dosing strategy below its maximum tolerated dose at 10 mg/kg IP × 3 days. PDT treatment was performed for 4 min. The dosing schedule was as follows: day 0, tumor implantation; day 10, 10% DMSO in normal saline (NS) administered to the vehicle control group, 10 mg/kg TMZ administered to the "TMZ alone" group and "combination" group; day 11, 10% DMSO in NS administered to the vehicle control group, 10 mg/kg TMZ administered to the "TMZ alone" and "combination" group, PDT treatment administered for a total of 4 min to the "PDT alone" group and the "combination" group; day 12, 10% DMSO in NS administered to the vehicle control group, 10 mg/kg TMZ administered to the "TMZ alone" group and the "combination" group.

The intracranial xenograft response was evaluated following the below protocols. The response of the intracranial xenografts to treatment was assessed in two ways. The primary end point was weight loss; once animals lost 15% of their body weight, they were removed from the study. A secondary end point was the percentage of increase in time to a specific neurologic end point (i.e., seizure activity, repetitive circling) or to moribund status. Statistical analysis was performed using

https://doi.org/10.1021/acsabm.2c00018
ACS Appl. Bio Mater. XXXX, XXX, XXX−XXX

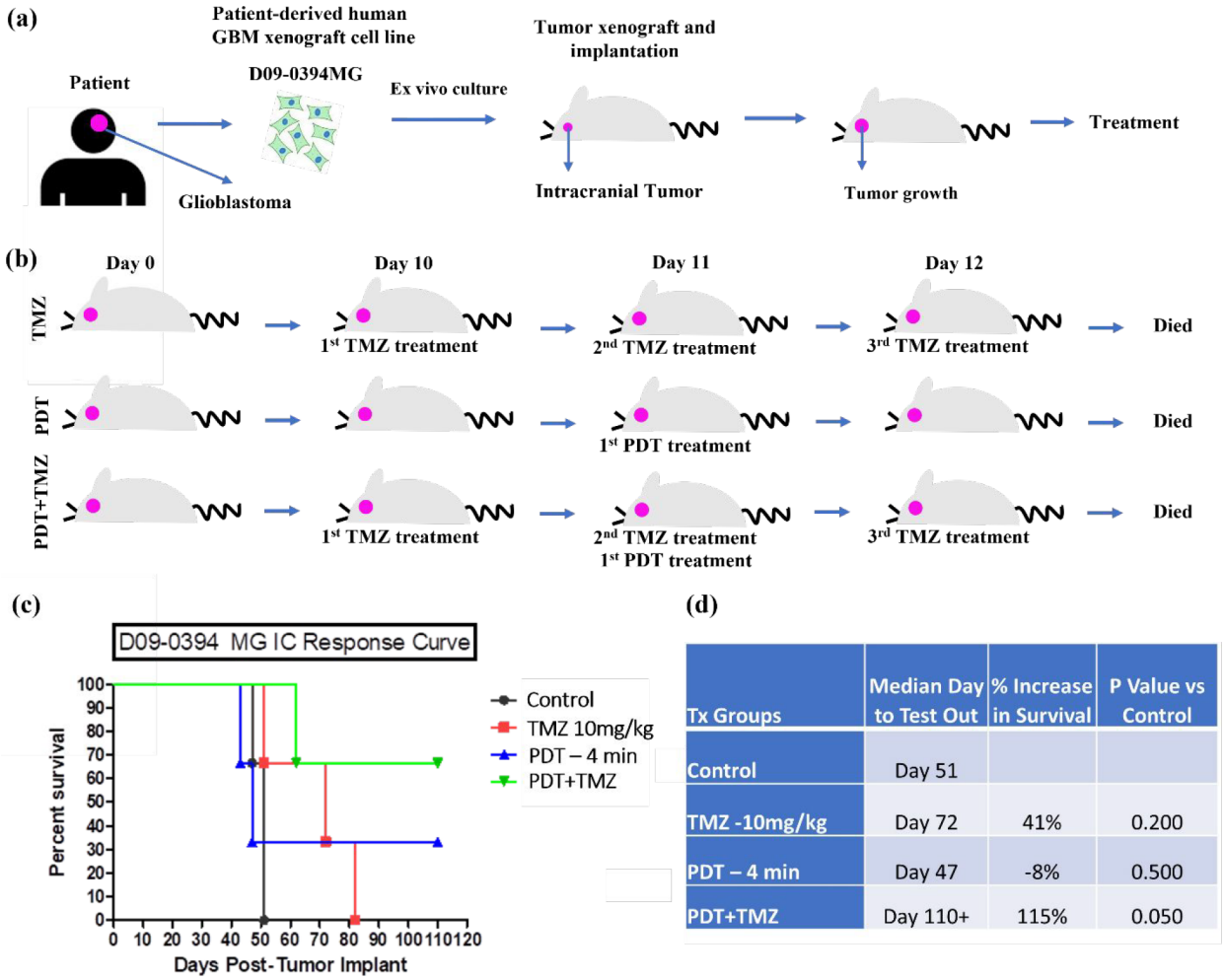

Figure 5. PDT drastically improves the survival of tumor-bearing mice. (a) Schematic illustration of the patient-derived xenograft model. Detailed protocols are illustrated in the Methods and Materials section. (b) Schematic illustration of experimental design. Detailed protocols are illustrated in the main text. (c) Mouse survival rate curve. (d) Quantitative analysis.

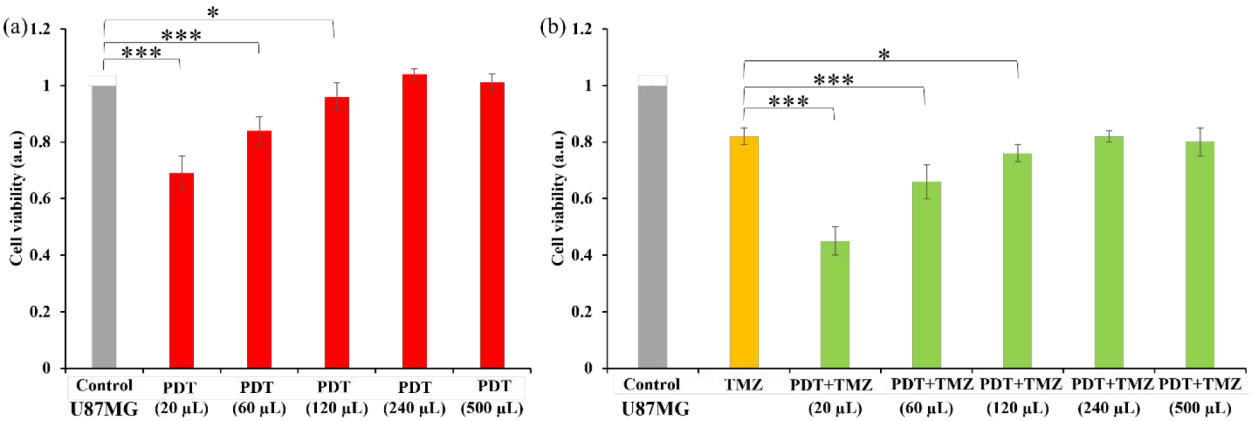

Figure 6. Medium volume affects PDT's effect on U87MG cells. (a) Different volumes of medium. PDT treatment lasted for 7 min. (b) PDT-TMZ treatment lasted for 7 min. A student's *t* test was performed, and statistical significance is indicated as * $p < 0.05$, ** $p < 0.01$, *** $p < 0.001$ ($n = 5$).

the Wilcoxon rank order test, as previously described.[23−25] All animals were observed twice daily for signs of distress or development of neurological symptoms, at which time they were removed from the study and euthanized. As shown in panels c and d in Figure 5, combination treatment of PDT +TMZ increased the mean survival days of the tumor-barrier mice by more than 100% compared to control group (110+ days vs 51 days). Different from previous studies, this work was the first demonstration of the human-originated primary xenografted tumor in vivo.

Factors that Affect PDT's Biological Effect. The volume of supernatant (medium) surrounding cells is a crucial parameter that affects the efficacy of PDT treatment. Here, we increased the volume of DMEM from 20 to 500 μL/well

https://doi.org/10.1021/acsabm.2c00018
ACS Appl. Bio Mater. XXXX, XXX, XXX−XXX

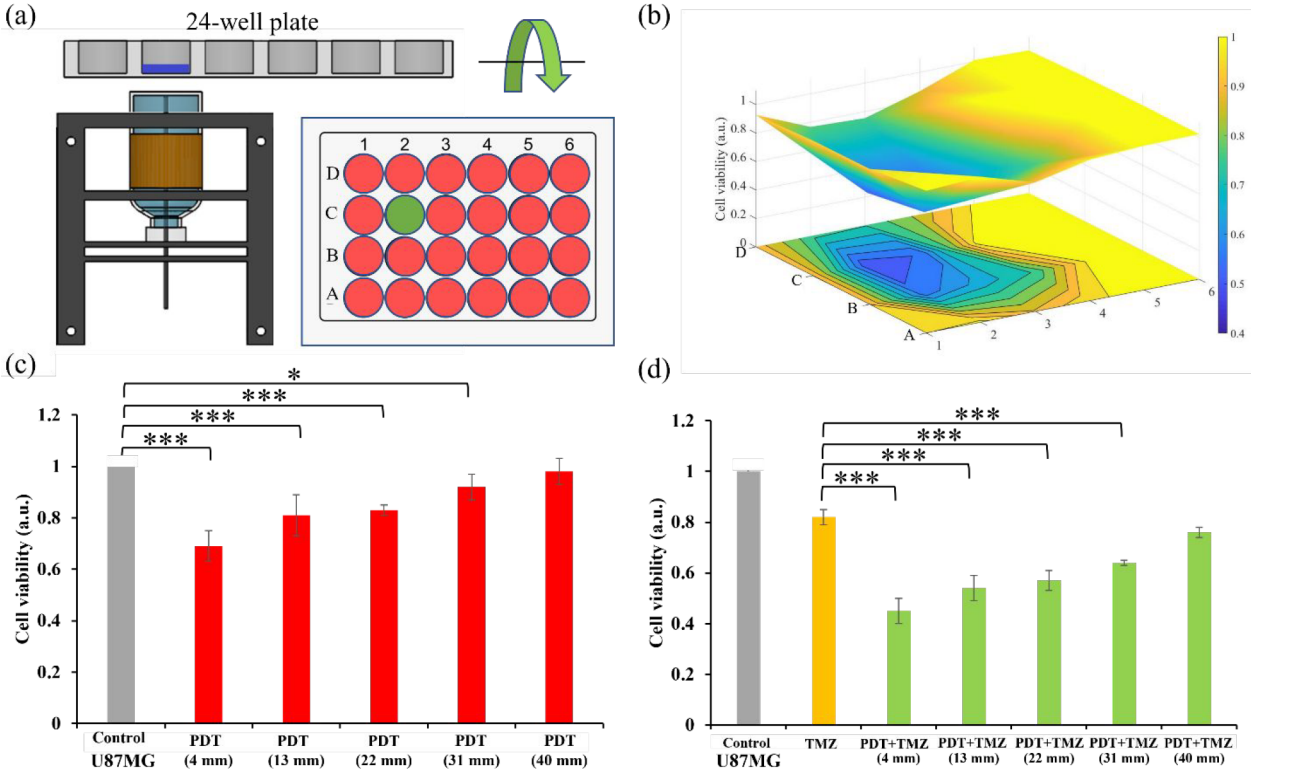

Figure 7. Relative spatial position between PDT and targets determines the antitumoral activity in U87MG cells. (a) Schematic illustration of setup. Treatment was performed on the well "2C" (in green). (b) PDT treatment (7 min) at a single well "2C" can affect numerous surrounding wells. Following the protocols in the literature,[12,22] the cell viabilities of all wells in a 24-well plate are presented in a 3D cell viability map using *MATLAB*. The projection of 3D maps is also presented here. (c) Cell viability of the well "2C" after PDT treatment (7 min), gap: 4 to 40 mm. (d) Cell viability of the well "2C" after PDT-TMZ treatment (7 min), gap: 4 to 40 mm. A student's *t* test was performed, and statistical significance is indicated as * $p < 0.05$, ** $p < 0.01$, *** $p < 0.001$ ($n = 5$).

during the treatment. To ensure identical culture conditions, we replaced the supernatant in all cases by 500 μL/well fresh DMEM after the treatment. As shown in Figure 6a, the PDT could strongly inhibit the cell viability only when the volume of medium was adequately small such as 20 μL/well. A large volume of medium such as 500 μL/well completely blocked PDT's killing effect. A similar trend was also observed in PDT-TMZ treatment. The enhanced cytotoxicity of TMZ by a PDT pretreatment could be completely inhibited when there was enough medium surrounding the cells (Figure 6b).

Unlike chemically based cold plasma treatment, which is fully determined by the concentration of reactive species, physically based cold plasma treatment is drastically affected by the relative spatial position between the cold plasma source and the target. Physical factors in cold plasma can affect an area much larger than the treated site. For instance, chemical factors such as reactive species cannot penetrate the walls in multiwell plates. Thus, only the plasma-touched single well will be affected.[12,22] In contrast, physical factors such as EM emission can penetrate dielectric materials such as polystyrene to affect many surrounding wells of the plasma-touched single well.[12,22] PDT treatment has a similar feature. As shown in Figure 7a, a PDT treatment on a single well of a 24-well plate could affect wells surrounding the treated well "2C". Here, all cell viability data on a 24-well plate were presented simultaneously using 3D cell viability maps, which has been used in previous studies.[12,22] Briefly, all absorbance at 570 nm in 24 wells was divided by the value of the control group. The obtained relative cell viability was drawn in 3D, in which the valley-shaped contour represented the largest growth inhibition that occurred at a specific well or area (Figure 7b). Obviously, the strongest growth inhibition occurred at the well "2C". Furthermore, the gap between the source and the target is another important factor affecting the PDT's performance. When the gap increased from 4 to 40 mm, the killing effect of both PDT and PDT-TMZ treatment drastically decreased (Figure 7c, d). Naturally, EM emission will have attenuation during the transmission from its source. Therefore, the gap's effect should be due to the natural EM emission's attenuation.

Metal can block the transmission of EM emissions from plasma sources.[12,22] We further investigated whether the exposure of a single well in PDT or PDT-TMZ treatment would still result in noticeable antitumoral activity. A copper sheet (McMaster-Carr, 9709k704) was used to cover the whole bottom of a 24-well plate during PDT treatment. The copper sheet was removed after the treatment, and cells were cultured under the standard conditions for 72 h. As shown in panels a and b in Figure 8, a copper sheet with a circular hole of 12 mm diameter could still allow EM emission to strongly affect U87MG cells just in the treated well but not in any other surrounding wells. When the PDT was moved away from cells, the antitumoral effect was weakened, the same trend observed in the treatment without copper sheets (Figure 8c, d). A complete copper sheet without a hole could completely inhibit the antitumoral effect (Figure 8e, f). The thickness (1 or 2 mm) of the copper sheet does not affect the antitumoral effect in both PDT and PDT-TMZ treatment (Figure 8g, h).

https://doi.org/10.1021/acsabm.2c00018
ACS Appl. Bio Mater. XXXX, XXX, XXX−XXX

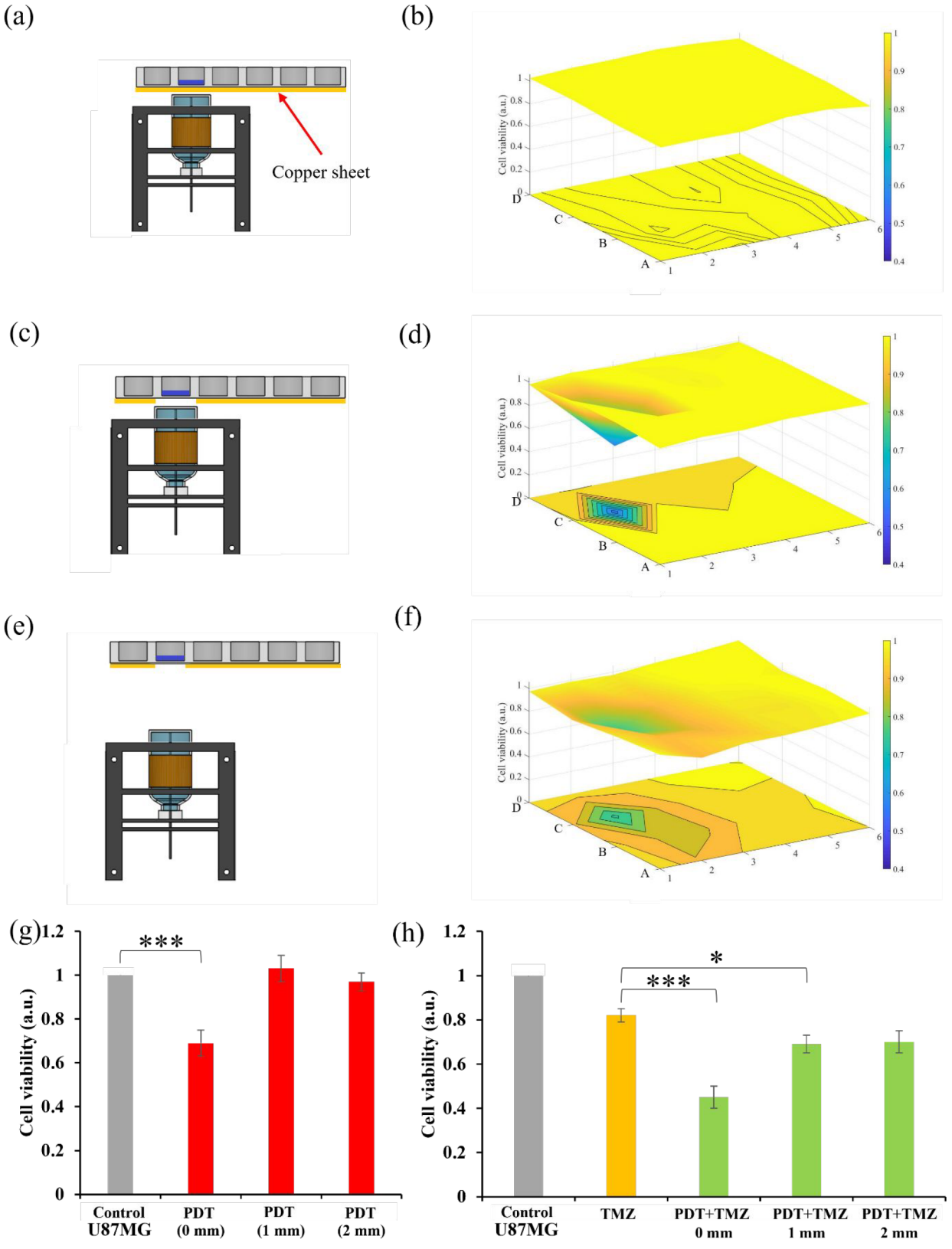

Figure 8. Copper sheet blocks PDT's physical effect on glioblastoma cells (U87MG). (a, b) Copper sheet can completely block PDT's effect on cells. Following the protocols in the literature,[12,22] the cell viabilities of all wells in a 24-well plate are presented in a 3D cell viability map. (c, d) Copper sheet just exposed to a single well "2C" in PDT treatment (gap 4 mm, 7 min). (e, f) Bigger gap between the PDT source and the target caused a weaker killing effect (gap 31 mm, 7 min). (g, h) Effect of copper sheet thickness (1, 2 mm) on PDT and PDT-TMZ (400 μM) treatment (7 min). Just the cell viabilities at the well "2C" are shown here. A student's t test was performed, and statistical significance is indicated as * $p < 0.05$, ** $p < 0.01$, *** $p < 0.001$ ($n = 5$).

https://doi.org/10.1021/acsabm.2c00018
ACS Appl. Bio Mater. XXXX, XXX, XXX−XXX

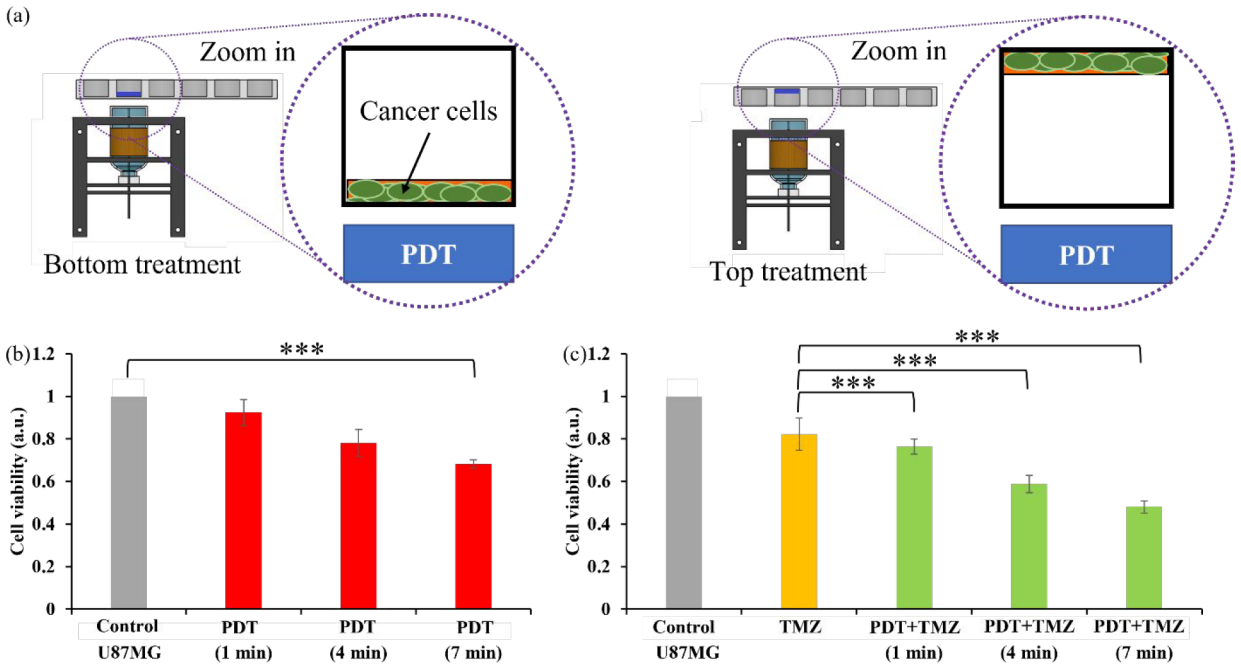

Figure 9. PDT treatment above U87MG cells. (a) Schematic illustration of PDT treatment with different directions. (b) Cell viability of the well "2C" after PDT treatment. (c) Cell viability of the well "2C" after PDT-TMZ treatment. A student's *t* test was performed, and the statistical significance is indicated as * $p < 0.05$, ** $p < 0.01$, *** $p < 0.001$ ($n = 5$).

Another important relative spatial position is where to locate the PDT treatment. In the above studies, all treatments were performed under the bottom of 24-well plates. EM emission from the PDT may be able to affect cells just above cells. As shown in Figure 9a, PDT treatment was performed on the inverted 12-well plate, which let the PDT treat cells from a different direction with a gap of 17 mm. It is found that PDT alone still decreased cell viability by 8, 22, and 32%, respectively (Figure 9b). Likewise, PDT-TMZ treatment achieved a noticeable antitumoral effect (Figure 9c). This trend clearly demonstrated that PDT treatment could be performed in different directions to achieve a similar anticancer effect, which may be an important guideline to design and use PDTs.

Multitime PDT Treatment. Multitime treatment of drugs has been used widely in chemotherapy and radiotherapy. However, in plasma medicine, a similar strategy has been rarely used. Here, we investigated the antitumoral efficacy of PDT using a multiple treatment strategy. 1.5×10^4 cells/well were seeded in a 24-well plate and cultured for 24 h before a PDT or PDT-TMZ treatment. For double treatment, PDT or PDT-TMZ treatment was performed on the first and the second day after the initial culture. The triple treatment followed the same protocols. The experimental conditions were identical to those previously described. Briefly, the overnighted supernatant was replaced by 20 μL/well fresh DMEM before PDT or PDT-TMZ treatment. After that, 20 μL/well fresh DMEM was immediately replaced by 500 μL/well DMEM or TMZ-DMEM (400 μM). For double and triple treatment, cells were cultured 48 and 24 h before the final cell viability assay, respectively.

Compared with a single treatment strategy, a multiple treatment drastically increased the killing effect on glioblastoma cells. For double treatment, PDT alone (1, 4, 7 min) caused an 8, 16, and 29% decrease, respectively, in the cell viability of U87MG cells. Although TMZ alone decreased cell viability by 19%, PDT-TMZ treatment (1, 4, 7 min) decreased cell viability by 19, 32, and 54%, respectively (Figure 10a). The triple treatment had a stronger antitumoral efficacy. PDT alone reduced cell viability by 6, 18, and 32%, respectively. PDT-TMZ treatment obtained a decreased cell viability by 16, 62, and 67%, respectively (Figure 10b). In contrast, these strongly enhanced effects have not been observed in the treated hTERT/E6/E7 cells. For double treatment, PDT alone (1, 4, 7 min) reduced cell viability by 4, 13, and 26%, respectively. PDT-TMZ treatment (1, 4, 7 min) increased cell viability by 26, 48, and 50%, respectively (Figure 10c). Triple treatment did not cause noticeable stronger cytotoxicity on hTERT/E6/E7 cells. PDT alone (1, 4, 7 min) reduced the cell viability of hTERT/E6/E7 cells by 10, 14, and 39%, respectively. PDT-TMZ treatment (1, 4, 7 min) decreased cell viability of hTERT/E6/E7 cells by 40, 50, and 51%, respectively (Figure 10d). In short, PDT selectively increased the cytotoxicity of TMZ on glioblastoma cells compared with normal astrocyte cells to some extent.

Coculture of Glioblastoma Cells with Astrocytes. Coculture of two cell lines provides an in vitro condition that is closer to the microenvironment in vivo than the single-cell line culture. Previous studies have demonstrated that chemically based cold plasma treatment has shown selectivity on the cocultured liver cancer cell line HepG2 and normal cell line L02 in vitro.[26] Here, we used a coculture system composed of glioblastoma U87MG cells and normal astrocyte hTERT/E6/E7 cells stained by CellTracker deep red dye and CellTracker green BODIPY dye, respectively (Figure 11a). The fluorescent emission at 660 and 529 nm was used to quantify the cell viability of U87MG cells and hTERT/E6/E7 cells, respectively.

The coculture cases demonstrated a much better selectivity toward U87MG cells than the above studies involving a single cell line. TMZ (400 μM) alone caused a similar but weak growth inhibition on both U87MG cells and hTERT/E6/E7

https://doi.org/10.1021/acsabm.2c00018
ACS Appl. Bio Mater. XXXX, XXX, XXX−XXX

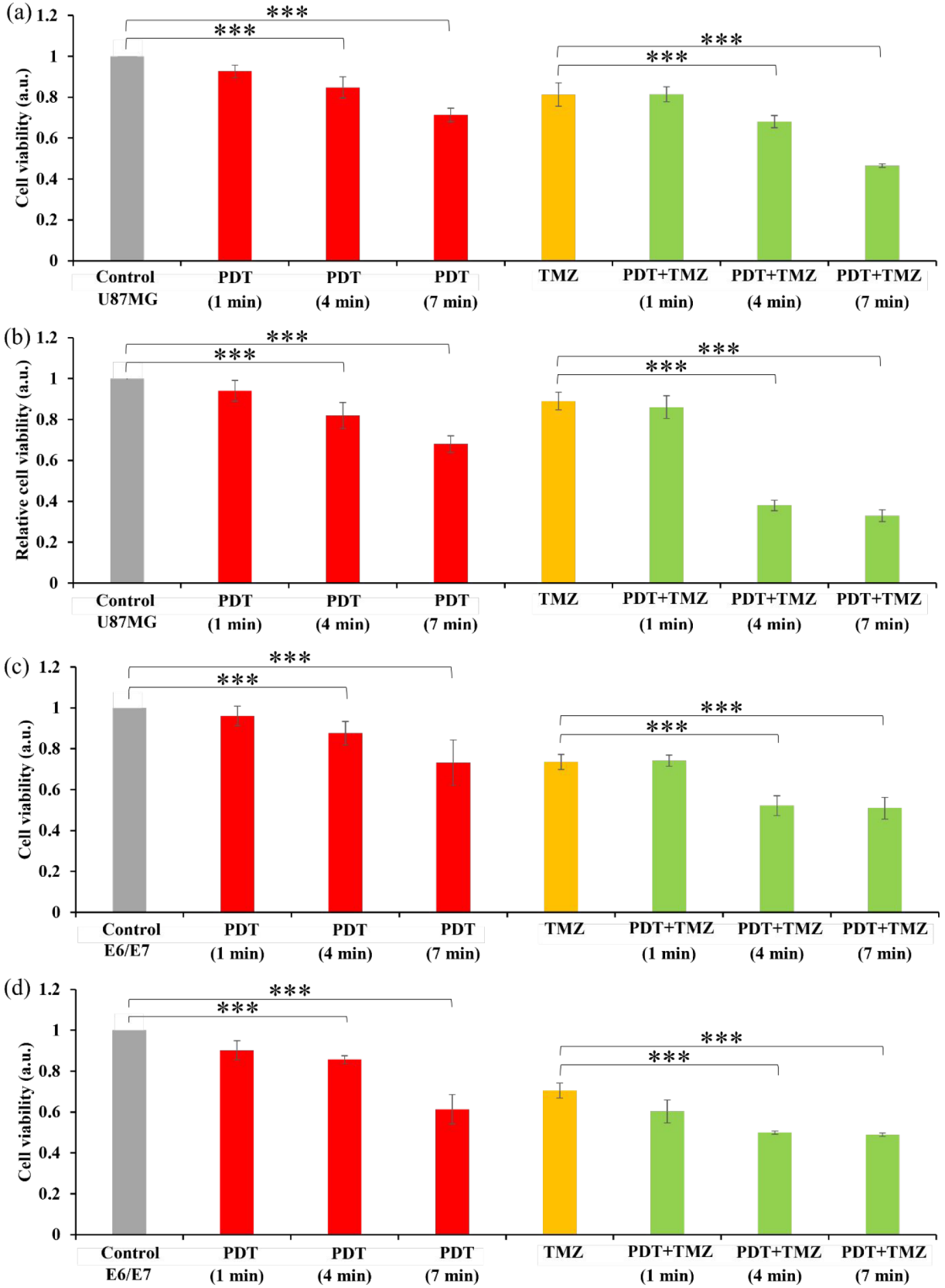

Figure 10. Multitime treatment selectively enhances antitumoral efficacy. Only the cell viability data of the well "2C" are shown here. (a) U87MG after a double treatment. (b) U87MG after a triple treatment. (c) hTERT/E6/E7 cells after a double treatment. (d) hTERT/E6/E7 cells after a triple treatment. A student's t test was performed, and the statistical significance is indicated as * $p < 0.05$, ** $p < 0.01$, *** $p < 0.001$ ($n = 5$).

cells (Figure 11b). PDT alone already showed a weak selectivity toward U87MG cells. As shown in Figure 11c, PDT alone decreased the viability of U87MG cells and hTERT/E6/E7 cells by 21 and 8%, respectively. In contrast,

https://doi.org/10.1021/acsabm.2c00018
ACS Appl. Bio Mater. XXXX, XXX, XXX−XXX

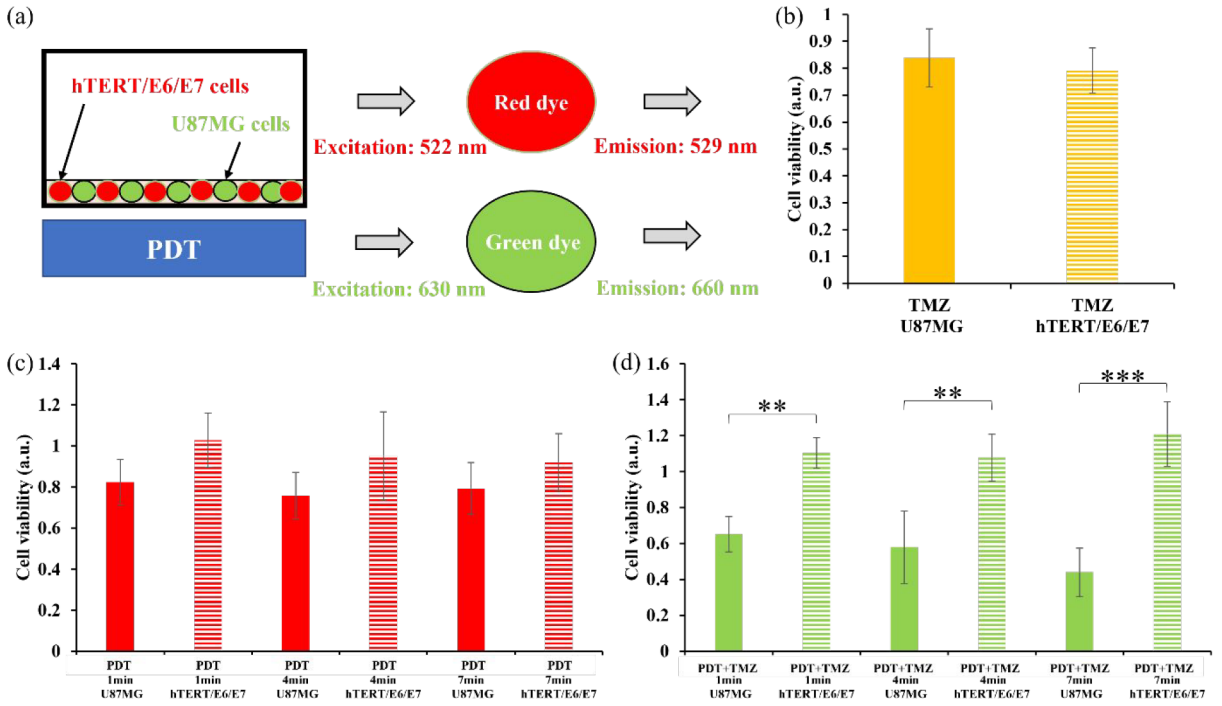

Figure 11. Selective antitumoral effect in a coculture system. (a) Schematic illustration of PDT treatment on U87MG cells and hTERT/E6/E7 cells. U87MG cells and hTERT/E6/E7 cells were stained by CellTracker Deep Red dye (Invitrogen, 25 μM) and CellTracker Green BODIPY Dye (Invitrogen, 10 mM), respectively. (b) TMZ effect on two cell lines. (c) PDT treatment (1, 4, 7 min) on two cell lines. (d) PDT-TMZ treatment (1, 4, 7 min) on two cell lines. Statistical significance is indicated as * $p < 0.05$, ** $p < 0.01$, *** $p < 0.001$ ($n = 5$)).

PDT-TMZ treatment obtained a strong selectivity toward U87MG cells. Seven minutes of PDT-TMZ treatment decreased the viability of U87MG cells by 55%. Surprisingly, the viability of hTERT/E6/E7 cells was increased by 20% compared with the control group. Such a drastic difference should be due to the better growth of normal cells when the neighboring cancer cells have been killed during PDT-TMZ treatment.

Cold Plasma Jet Treatment. Cold plasma jet is the most widely used cold plasma source in plasma medicine-related studies.[27] Here, we investigated whether physically based cold plasma treatment could enhance the cytotoxicity of TMZ on glioblastoma cell line A172. This cold plasma jet source has been used many times in previous studies (Figure 12a). The detailed introduction can be found in previous references.[28,29] Physically based cold plasma treatment uses a cold plasma jet to affect cells by blocking the contact between all chemical factors and cells.[12,14,22] One simple approach was using a cold plasma jet to treat the bottom of an inverted multiwell plate or dishes, in which the bottom of the plate or dish will block all reactive species.[12,14,22] In fact, only this strategy has been used so far. Another potential approach is treating cells from the lid rather than from the bottom. However, this strategy has no killing effect because there is too large of an air gap between the lid and the target, which will cause a very weak EM effect on cells' viability.

Here, we compared two strategies of physically based cold plasma jet treatment: the treatment from the bottom of a 12-well plate and the treatment above the lid of a 12-well plate (Figure 12b). A172 cells at a concentration of 7.5×10^4 cells/well were seeded in a 12-well plate and cultured for 24 h before cold plasma jet treatment. The overnighted supernatant was removed before treatment. Subsequently, 1 mL/well fresh DMEM or TMZ-DMEM (80, 200, and 300 μM) was immediately added to culture cells for 72 h before the final MTT assay. It was found that cold plasma jet treatment on the lid with or without TMZ did not show any impact on A172 cells (Figure 12c, d). Cold plasma jet treatment on the bottom strongly inhibits the growth of A172 cells (Figure 12e). However, cold plasma jet treatment did not enhance the cytotoxicity of TMZ (80, 200, and 300 μM) on A172 cells (Figure 12f–h). The cold plasma jet alone caused a strong killing effect on A172 cells. In contrast, the PDT alone just caused a weak effect. However, use of a PDT rather than a cold plasma jet can enhance the cytotoxicity of TMZ on glioblastoma cells. Thus, the biological effect of physical factors from cold plasma jet was different from that of PDT.

DISCUSSIONS

Traditional plasma medicine is based on the biological response to chemical components in a cold plasma source, such as a cold plasma jet.[5,6] As a result, direct contact between the cold plasma and the target is always necessary, particularly for the case involving a solution layer covering cells or tissues during the treatment.[30] This is a limitation of chemically based cold plasma treatment. In contrast, physical factors in cold plasma can penetrate a physical barrier such as a dielectric material and affect cells in a contactless way.[12−14,31] This distinct nature shines a light on using the physically based cold plasma treatment as a novel noninvasive modality. Here, PDT not only demonstrates its strong antitumoral activity in GBM by a contactless treatment method but also demonstrates its ability to selectively enhance the therapeutic performance of the widely used alkylating agent in GBM, TMZ. These results suggest that it is possible to build a cold plasma source to improve the current chemotherapy efficacy of glioblastoma in a noninvasive way. One way to bring this into the clinic is

https://doi.org/10.1021/acsabm.2c00018
ACS Appl. Bio Mater. XXXX, XXX, XXX−XXX

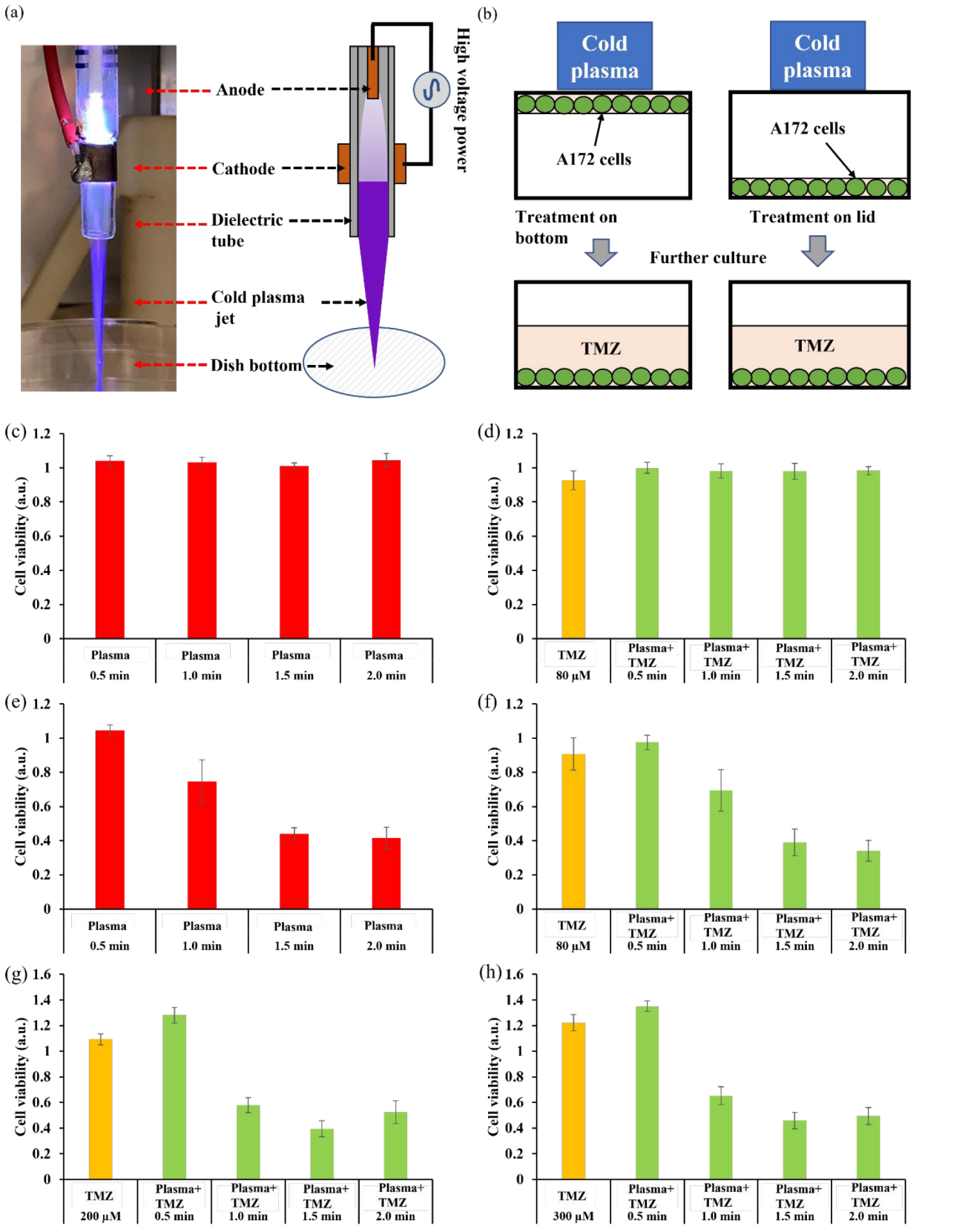

Figure 12. Physically based cold plasma jet treatment on glioblastoma cells (A172). (a) Cold plasma jet source and basic structural illustration. (b) Two treatment strategies. (c) Cold plasma jet treatment on the lid. (d) Cold plasma jet treatment on the lid followed by TMZ treatment (80 μM). (e) Cold plasma jet treatment on the bottom. (f) Cold plasma jet treatment on the bottom followed by TMZ treatment (80 μM). (g,h) Cold plasma jet treatment on the bottom followed by TMZ treatment (200 μM, 300 μM) (n = 3).

https://doi.org/10.1021/acsabm.2c00018
ACS Appl. Bio Mater. XXXX, XXX, XXX−XXX

through the development or use of a multifunctional therapeutic helmet.

This study provides several guidelines to use PDT in clinical practice. (1) PDT 's biological effect will be counteracted when too much liquid surrounds cells or tissues. This feature has been widely observed in the physically based cold plasma treatment.[12−14,31] (2) Like the chemically based cold plasma treatment, a smaller gap between PDT source and target will cause a stronger killing effect. (3) Conductive materials such as copper sheet can completely block the biological effect of PDT treatment by blocking the transmission of EM emission. (4) PDT can affect the biological targets such as cells from multiple directions, which is also a typical feature of physically based cold plasma treatment. (5) Multiple treatments on cells causes a much stronger killing effect than a single treatment.

PDT shows advantages over the existing physically based cold plasma treatment. As we demonstrated, just 7 min of PDT treatment can achieve a strong efficacy. Although the cold plasma jet is also a nonequilibrium plasma, it has not shown any enhancement on TMZ's cytotoxicity. On the contrary, a cold plasma jet alone can cause a much stronger killing effect than PDT. Thus, a cold plasma jet is more likely to kill glioblastoma cells rather than sensitizing it to TMZ. Such different cellular responses can be regarded as an advantage of PDT over the cold plasma jet source.

The underlying mechanism is still largely an open question. First of all, the effective EM emission range to cause these growth inhibitions and selective enhancement of the drug's cytotoxicity is still unknown. What is the difference between the PDT source and the cold plasma jet source in terms of EM emission or other physical factors? In addition, it is completely unknown why there is a selective biological effect of cold plasma treatment, which may be due to the distinct biological response of cancer cells and normal cells to the EM effect at a specific wavelength range. A satisfactory answer to these questions is crucial for the application of PDT in plasma medicine. Because TMZ mainly affects the DNA-pair pathways in glioblastoma cells, the EM emission from PDT may selectively affect these pathways or main modulators in glioblastoma cells, such as DNA repair protein O6−methylguanine−DNA methyltransferase.[32] Despite these confusions, the published studies based on physical factors in cold plasma clearly demonstrate that plasma medicine is not a field solely based on reactive species.

CONCLUSIONS

In summary, we designed here a novel cold plasma source, a PDT, which will affect cells only by its physical factors. We demonstrated the strong antitumoral capability of the PDT in vitro and in vivo. More importantly, the PDT drastically and selectively enhanced the cytotoxicity of TMZ on two glioblastoma cell lines U87MG and A172 but less so on astrocyte cell line hTERT/E6/E7, particularly in the coculture experiment. These results suggest the potentiality of using PDTs in glioblastoma therapy as a noninvasive and safe modality. Furthermore, PDTs do not require a continuous noble gas supply compared with traditional cold plasma sources, which drastically decreases operational costs. More attractively, the noble gas is in an isolated and sealed space in the PDT. Thus, environmental factors will not interfere with such a source and achieve a much better operational stability compared with the cold plasma jet source. All these features shine a light on using PDTs as portable medical devices.

ASSOCIATED CONTENT

Supporting Information

The Supporting Information is available free of charge at https://pubs.acs.org/doi/10.1021/acsabm.2c00018.

Figure S1, tumor implantation coordinates shown on a mouse (PDF)

AUTHOR INFORMATION

Corresponding Authors

Dayun Yan − *Department of Mechanical and Aerospace Engineering, George Washington University, Washington, District of Columbia 20052, United States;* orcid.org/0000-0002-9801-021X; Email: ydy2012@gwmail.gwu.edu

Michael Keidar − *Department of Mechanical and Aerospace Engineering, George Washington University, Washington, District of Columbia 20052, United States*; Email: keidar@gwu.edu

Authors

Xiaoliang Yao − *Department of Mechanical and Aerospace Engineering, George Washington University, Washington, District of Columbia 20052, United States*

Li Lin − *Department of Mechanical and Aerospace Engineering, George Washington University, Washington, District of Columbia 20052, United States*

Jonathan H. Sherman − *WVU Medicine−Berkeley Medical Center, West Virginia University, Martinsburg, West Virginia 25041, United States*

Katherine B. Peters − *Departments of Neurology and Neurosurgery, Duke University School of Medicine, Durham, North Carolina 27710, United States*

Stephen T. Keir − *Departments of Neurology and Neurosurgery, Duke University School of Medicine, Durham, North Carolina 27710, United States*

Complete contact information is available at: https://pubs.acs.org/10.1021/acsabm.2c00018

Author Contributions

†X.Y. and D.Y. contributed equally to this manuscript.

Notes

The authors declare no competing financial interest.

The data that support the findings of this study are available from the corresponding author upon reasonable request.

ACKNOWLEDGMENTS

This research was funded by National Science Foundation grant, Grant 1747760.

REFERENCES

(1) Tendero, C.; Tixier, C.; Tristant, P.; Desmaison, J.; Leprince, P. Atmospheric Pressure Plasmas: A Review. *Spectrochimica Acta - Part B Atomic Spectroscopy* **2006**, *61* (1), 2−30.

(2) Laroussi, M.; Akan, T. Arc-Free Atmospheric Pressure Cold Plasma Jets: A Review. *Plasma Processes and Polymers* **2007**, *4* (9), 777−788.

(3) Keidar, M. A Prospectus on Innovations in the Plasma Treatment of Cancer. *Physics of Plasmas* **2018**, *25* (8), 083504.

(4) Lu, X. P.; Ostrikov, K. K. Guided Ionization Waves: The Physics of Repeatability. *Applied Physics Reviews* **2018**, *5* (3), 031102.

(5) Lu, X.; Naidis, G. V.; Laroussi, M.; Reuter, S.; Graves, D. B.; Ostrikov, K. Reactive Species in Non-Equilibrium Atmospheric-Pressure Plasmas: Generation, Transport, and Biological Effects. *Phys. Rep.* **2016**, *630*, 1−84.

(6) Graves, D. B. The Emerging Role of Reactive Oxygen and Nitrogen Species in Redox Biology and Some Implications for Plasma Applications to Medicine and Biology. *J. Phys. D: Appl. Phys.* **2012**, *45* (45), 263001−263042.
(7) Bauer, G.; Graves, D. B. Mechanisms of Selective Antitumor Action of Cold Atmospheric Plasma-Derived Reactive Oxygen and Nitrogen Species. *Plasma Processes and Polymers* **2016**, *13* (12), 1157−1178.
(8) Keidar, M. Plasma for Cancer Treatment. *Plasma Sources Science and Technology* **2015**, *24* (3), 033001.
(9) Yan, D.; Sherman, J. H.; Keidar, M. Cold Atmospheric Plasma, a Novel Promising Anti-Cancer Treatment Modality. *Oncotarget* **2017**, *8*, 15977.
(10) Graves, D. B. Mechanisms of Plasma Medicine: Coupling Plasma Physics, Biochemistry, and Biology. *IEEE Transactions on Radiation and Plasma Medical Sciences* **2017**, *1* (4), 281−292.
(11) Keidar, M.; Yan, D.; Beilis, I. I.; Trink, B.; Sherman, J. H. Plasmas for Treating Cancer: Opportunities for Adaptive and Self-Adaptive Approaches. *Trends Biotechnol.* **2018**, *36*, 586−593.
(12) Yan, D.; Wang, Q.; Adhikari, M.; Malyavko, A.; Lin, L.; Zolotukhin, D. B.; Yao, X.; Kirschner, M.; Sherman, J. H.; Keidar, M. A Physically Triggered Cell Death via Transbarrier Cold Atmospheric Plasma Cancer Treatment. *ACS Appl. Mater. Interfaces* **2020**, *12* (31), 34548−34563.
(13) Wang, Q.; Malyavko, A.; Yan, D.; Lamanna, O. K.; Hsieh, M. H.; Sherman, J.; Keidar, M. A Comparative Study of Cold Atmospheric Plasma Treatment, Chemical versus Physical Strategy. *J. Phys. D: Appl. Phys.* **2021**, *54*, 095207.
(14) Malyavko, A.; Yan, D.; Wang, Q.; Klein, A. L.; Patel, K. C.; Sherman, J. H.; Keidar, M. Cold Atmospheric Plasma Cancer Treatment, Direct versus Indirect Approaches. *Materials Advances* **2020**, *1* (6), 1494−1505.
(15) Lin, L.; Keidar, M. A Map of Control for Cold Atmospheric Plasma Jets: From Physical Mechanisms to Optimizations. *Applied Physics Reviews* **2021**, *8* (1), 011306.
(16) Wang, X.; Song, J.; Liu, J.; Wang, Z. Direct-Current Nanogenerator Driven by Ultrasonic Waves. *Science* **2007**, *316* (5821), 102−105.
(17) Ohgaki, H.; Kleihues, P. The Definition of Primary and Secondary Glioblastoma. *Clinical cancer research* **2013**, *19* (4), 764−772.
(18) Lee, S. Y. Temozolomide Resistance in Glioblastoma Multiforme. *Genes & Diseases* **2016**, *3* (3), 198−210.
(19) Yung, W. K. A.; Albright, R. E.; Olson, J.; Fredericks, R.; Fink, K.; Prados, M. D.; Brada, M.; Spence, A.; Hohl, R. J.; Shapiro, W.; et al. A Phase II Study of Temozolomide vs. Procarbazine in Patients with Glioblastoma Multiforme at First Relapse. *Br. J. Cancer* **2000**, *83*, 588−593.
(20) Bae, S. H.; Park, M.; Lee, M. M.; Kim, T. M.; Lee, S.; Cho, S. Y.; Kim, Y.; Kim, Y. J.; Park, C.; Kim, C. Toxicity Profile of Temozolomide in the Treatment of 300 Malignant Glioma Patients in Korea. *Journal of Korean Medical Science* **2014**, *29*, 980−984.
(21) Fu, W.; You, C.; Ma, L.; Li, H.; Ju, Y.; Guo, X.; Shi, S.; Zhang, T.; Zhou, R.; Lin, Y. Enhanced Efficacy of Temozolomide Loaded by a Tetrahedral Framework DNA Nanoparticle in the Therapy for Glioblastoma. *ACS Appl. Mater. Interfaces* **2019**, *11* (43), 39525−39533.
(22) Yan, D.; Wang, Q.; Malyavko, A.; Zolotukhin, D. B.; Adhikari, M.; Sherman, J. H.; Keidar, M. The Anti-Glioblastoma Effect of Cold Atmospheric Plasma Treatment: Physical Pathway v. s. Chemical Pathway. *Sci. Rep.* **2020**, *10* (1), 11788.
(23) Carlson, B. L.; Pokorny, J. L.; Schroeder, M. A.; Sarkaria, J. N. Establishment, Maintenance and in Vitro and in Vivo Applications of Primary Human Glioblastoma Multiforme (GBM) Xenograft Models for Translational Biology Studies and Drug Discovery. *Current protocols in pharmacology* **2011**, *52*, 14−16.
(24) Keir, S. T.; Hausheer, F.; Lawless, A. A.; Bigner, D. D.; Friedman, H. S. Therapeutic Activity of 7-[(2-Trimethylsilyl)Ethyl)]-20 (S)-Camptothecin against Central Nervous System Tumor-Derived Xenografts in Athymic Mice. *Cancer Chemotherapy and Pharmacology* **2001**, *48* (1), 83−87.
(25) Gehan, E. A. A Generalized Two-Sample Wilcoxon Test for Doubly Censored Data. *Biometrika* **1965**, *52* (34), 650−653.
(26) Duan, J.; Lu, X.; He, G. The Selective Effect of Plasma Activated Medium in an *in Vitro* Co-Culture of Liver Cancer and Normal Cells. *J. Appl. Phys.* **2017**, *121* (1), 013302.
(27) Lu, X.; Laroussi, M.; Puech, V. 2012. On Atmospheric-Pressure Non-equilibrium Plasma Jets and Plasma Bullets. *Plasma Sources Science and Technology* **2012**, *21* (3), 034005.
(28) Yan, D.; Talbot, A.; Nourmohammadi, N.; Cheng, X.; Canady, J.; Sherman, J.; Keidar, M. Principles of Using Cold Atmospheric Plasma Stimulated Media for Cancer Treatment. *Sci. Rep.* **2015**, *5*, 18339.
(29) Yan, D.; Lin, L.; Xu, W.; Nourmohammadi, N.; Sherman, J.; Keidar, M. Cold Plasma-Based Control of the Activation of Pancreatic Adenocarcinoma Cells. *J. Phys. D: Appl. Phys.* **2019**, *52* (44), 445202.
(30) Stupp, R.; Wong, E. T.; Kanner, A. A.; Steinberg, D.; Engelhard, H.; Heidecke, V.; Kirson, E. D.; Taillibert, S.; Liebermann, F.; Dbalý, V.; Ram, Z. NovoTTF-100A versus Physician's Choice Chemotherapy in Recurrent Glioblastoma: A Randomised Phase III Trial of a Novel Treatment Modality. *Eur. J. Cancer* **2012**, *48* (14), 2192−2202.
(31) Salzberg, M.; Kirson, E.; Palti, Y.; Rochlitz, C. A Pilot Study with Very Low-Intensity, Intermediate-Frequency Electric Fields in Patients with Locally Advanced and/or Metastatic Solid Tumors. *Onkologie* **2008**, *31* (7), 362−365.
(32) Yoshimoto, K.; Mizoguchi, M.; Hata, N.; Murata, H.; Hatae, R.; Amano, T.; Nakamizo, A.; Sasaki, T. Complex DNA Repair Pathways as Possible Therapeutic Targets to Overcome Temozolomide Resistance in Glioblastoma. *Front. Oncol.* **2012**, *2*, 186.

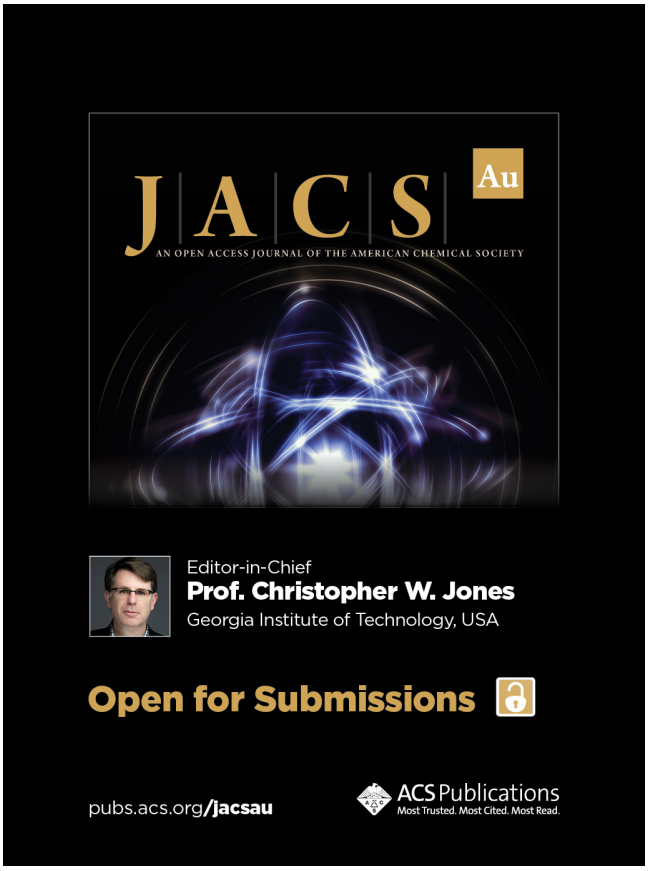

https://doi.org/10.1021/acsabm.2c00018
ACS Appl. Bio Mater. XXXX, XXX, XXX−XXX